

Elucidation of the Contribution of Active Site and Exosite Interactions to Affinity and Specificity of Peptidyl Serine Protease Inhibitors Using Non-Natural Arginine Analogs^[S]

Masood Hosseini, Longguang Jiang, Hans Peter Sørensen, Jan K. Jensen, Anni Christensen, Sarah Fogh, Cai Yuan, Lisbeth M. Andersen, Mingdong Huang, Peter A. Andreasen, and Knud J. Jensen

Department of Natural Sciences and Environment, Faculty of Life Sciences, University of Copenhagen, Copenhagen, Denmark (M.H., K.J.J.); Department of Molecular Biology, Aarhus University, Aarhus, Denmark (M.H., H.P.S., J.K.J., A.C., S.F., L.M.A., P.A.A.); and Fujian Institute of Research on the Structure of Matter, Chinese Academy of Sciences, Fuzhou, China (L.J., C.Y., M.H.)

Received March 19, 2011; accepted June 30, 2011

ABSTRACT

There is increasing interest in developing peptides for pharmacological intervention with pathophysiological functions of serine proteases. From phage-displayed peptide libraries, we previously isolated peptidyl inhibitors of urokinase-type plasminogen activator, a potential target for intervention with cancer invasion. The two peptides, upain-1 (CSWRGLENHRMC) and mupain-1 (CPAYSRYLDC), are competitive inhibitors of human and murine urokinase-type plasminogen activator, respectively. Both have an Arg as the P1 residue, inserting into the S1 pocket in the active site of the enzymes, but their specificity depends to a large extent on interactions outside the enzymes' active sites, so-called exosite interactions. Here we describe upain-2 (CSWRGLENHAAC) and the synthesis of a number of upain-2 and mupain-1 variants in which the P1 Arg was substituted with novel non-natural

Arg analogs and achieved considerable improvement in the affinity of the peptides to their targets. Using chimeras of human and murine urokinase-type plasminogen activator as well as X-ray crystallography, we delineated the relative contribution of the P1 residue and exosite interactions to the affinity and specificity of the inhibitors for their target enzyme. The effect of inserting a particular non-natural amino acid into the P1 position is determined by the fact that changes in interactions of the P1 residue in the S1 pocket lead to changed exosite interactions and vice versa. These findings are of general interest when the affinities and specificities of serine protease inhibitors to be used for pharmacological intervention are considered and could pave the way for potential drug candidates for the treatment of cancer.

Introduction

In recent years, peptides have attracted renewed interest as drug candidates. Most often, they display high specificity,

comparable with those of monoclonal antibodies, but because of their smaller size are amenable to chemical modification. They have predictable absorption, distribution, metabolism, and excretion properties and display a general absence of drug-drug interactions. Although peptides are labile to proteolysis, stable forms can be developed by chemical modification. Moreover, new delivery methods have enabled the formulation of peptide preparations suitable for in vivo use (for review, see Jorgensen and Nielsen, 2009).

One important class of potential therapeutic targets is the trypsin family (clan SA) of serine proteases, which has many pathophysiological functions. Therefore, the interest in serine protease inhibitors is increasing (for review, see Walker and Lynas, 2001). Moreover, serine proteases are classic

This work was supported by the National Natural Science Foundation of China [Grants 30811130467, 30973567, 30770429]; the Danish National Research Foundation [Grant 26-331-6]; the Lundbeck Foundation [Grant R19-A2173]; the Danish Cancer Society [Grant DP 07043, DP 08001]; the Danish Research Agency [Grant 272-06-0518]; and the Novo Nordisk Foundation [Grant R114-A11382].

All authors are affiliated with the Danish-Chinese Centre for Proteases and Cancer (<http://www.proteasesandcancer.org>).

Article, publication date, and citation information can be found at <http://molpharm.aspetjournals.org>.
doi:10.1124/mol.111.072280.

[S] The online version of this article (available at <http://molpharm.aspetjournals.org>) contains supplemental material.

ABBREVIATIONS: uPA, urokinase-type plasminogen activator; Fmoc, 9H-fluoren-9-ylmethoxycarbonyl; Dap, L-2,3-diaminopropionic acid; Boc, di-tert-butyl dicarbonate; HPLC, high-performance liquid chromatography; HBTU, N-[(1H-benzotriazol-1-yl)(dimethylamino)methylene]-N-methylmethanaminium hexafluorophosphate N-oxide; TFA, trifluoroacetic acid; HOBt, N-hydroxybenzotriazole; HOAt, 1-hydroxy-7-azabenzotriazole; DIPEA, N,N-diisopropylethylamine; NMP, N-methyl-2-pyrrolidone; Alloc, allyloxycarbonyl; HRMS, high-resolution mass spectrometry; ES, electrospray; Cbz, carboxybenzyl; Fmoc-OSu, 9-fluorenylmethoxycarbonyl-N-hydroxysuccinimide; MS, mass spectrometry; wt, wild-type; S-2444, pyro-Glu-Gly-Arg-p-nitroanilide; PDB, Protein Data Bank.

subjects for studies of catalytic and inhibitory mechanisms (for review, see Branden and Tooze, 1991). However, the human genome contains approximately 200 serine protease genes (for review, see Puente et al., 2008). Although different serine proteases have different substrate specificities, the catalytic site architectures are highly similar. Achieving sufficient specificity is, therefore, a challenge of utmost importance when serine protease inhibitors are developed. Development of small molecule inhibitors has proved to be a daunting task (for review, see Rockway et al., 2002). To develop inhibitors with better specificity, a number of peptidic serine protease inhibitors have recently been isolated by screening phage-displayed peptide libraries, including inhibitors of chymotrypsin (Krook et al., 1997–1998), factor VIIa (Dennis et al., 2000), prostate-specific antigen (Wu et al., 2000), kallikrein-2 (Hekim et al., 2006; Heinis et al., 2009), mannose-binding lectin-associated serine protease-1 and -2 (Kocsis et al., 2010), furins (Hajdin et al., 2010), and isoforms of trypsin (Wu et al., 2010).

One example of a serine protease that is a potential drug target is urokinase-type plasminogen activator (uPA), which catalyzes the conversion of plasminogen to the active protease plasmin. Plasmin in turn catalyzes directly the degradation of extracellular matrix proteins. Up-regulation of uPA is implicated in tissue remodeling in several pathological conditions. In particular, uPA is central to the invasive capacity of malignant tumors (for review, see Andreasen et al., 2000). We previously isolated two peptides, one (upain-1, CSWRGLENHRMC) being an inhibitor of human uPA (Hansen et al., 2005) and the other (mupain-1, CPAYSRYLDC) being an inhibitor of murine uPA (Andersen et al., 2008). Both are constrained in a circular form by a disulfide bridge. Both are highly specific for the target enzyme against which they were selected. Thus, upain-1 binds approximately 500-fold better to human uPA than to murine uPA, whereas mupain-1 binds more than 2000-fold better to murine uPA than to human uPA. Both bind very selectively to uPA compared with other serine proteases from the same species (Hansen et al., 2005; Andersen et al., 2008). Analysis of the inhibitory mechanism showed that both upain-1 and mupain-1 are competitive inhibitors of their target enzymes (Hansen et al., 2005; Andersen et al., 2008). Site-directed mutagenesis (Hansen et al., 2005; Andersen et al., 2008) and X-ray crystal structure analysis (Zhao et al., 2007) showed that Arg4 of upain-1 and Arg6 of mupain-1 are the P1¹ residues of these peptides, i.e., are inserted into the enzymes' S1 or specificity pocket, the primary interaction site between substrate and enzyme. In the case of upain-1, X-ray crystal structure analysis showed that the side-chain of the peptide's Glu7 blocks the enzyme's oxyanion hole (Zhao et al., 2007). Upain-1 and mupain-1 thus directly occupy the structures of the active sites, which are essential for the catalytic machinery for peptide bond hydrolysis (for review, see Hedstrom, 2002). However, the great specificity of both peptides is achieved by a large interaction area, involving not only the active sites but also surface-exposed loops specific for individual proteases (i.e., exosite interactions).

¹ P1, P2, P3, P4, etc. and P1', P2', P3', etc. are of the nomenclature of Schechter and Berger (Abramowitz et al., 1967) and denote those residues on the amino-terminal and carboxyl sides of the scissile bond (P1–P1'), respectively. The corresponding binding sites in the active sites of the enzymes are referred to as S1, S2, S3, S4, etc., and S'1, S'2, S'3, etc.

Upain-1 inhibits human uPA with a K_i of approximately 40 μM at 37°C. Mupain-1 has a considerably higher, although still not quite satisfactory, affinity to murine uPA, with a K_i of approximately 0.4 μM at 37°C. In an effort to engineer the peptides to higher affinity while maintaining specificity and to understand enzyme-inhibitor interactions, we have first made two amino acid substitutions in upain-1 to obtain upain-2 and, second, substituted the P1 L-Arg residues in mupain-1 and upain-2 with a variety of novel non-natural arginine analogs. By testing different P1 residues in uPA variants with different S1 pockets and different surface loops, we have evaluated the importance of S1 pocket interactions versus exosite interactions for the affinity and specificity of the peptides.

Materials and Methods

General. Chemicals were purchased from Sigma-Aldrich (St. Louis, MO), Iris Biotech GmbH (Marktredwitz, Germany) and Rapp Polymere GmbH (Tübingen, Germany) and used without further purification unless otherwise stated. Fmoc-HArg(Pbf)-OH, Fmoc-L-Dap-N-amidine(*N*, *N'*-di-Boc)-OH, Fmoc-L-NorArg(*N*, *N'*-di-Boc)-OH, Fmoc-citrulline-OH, Fmoc-L-4-guanidino-phenylalanine(*N*, *N'*-di-Boc)-OH, Fmoc-L-2, 3-diaminopropionic acid-OH, Fmoc-L-bishomoarginine(Pmc)-OH, Fmoc-D-Arg(2,2,4,6,7-pentamethyldihydrobenzofuran-5-sulfonyl)-OH, Fmoc-L-Ala-4-piperidyl(Alloc)-OH, *N*- α -(Fmoc)-3-(3-pyridyl)-L-alanine, and Fmoc-L-canavanine(Boc)-OH were commercially available. 4-(2,3-Bis(*tert*-butoxycarbonyl)guanidino)benzoic acid was synthesized according to a procedure published previously (Kayser et al., 2007). NMR was performed using a Bruker Avance 300 spectrometer. Analytical HPLC was performed on a UltiMate 3000 (Dionex, Sunnyvale, CA), using a Gemini 110 Å C18 column (3 μm , 4.6 \times 50 mm; Phenomenex, Torrance, CA) with a flow rate of 1.0 ml/min and a linear gradient going from 95% H₂O–5% acetonitrile with 0.1% HCOOH to 100% acetonitrile with 0.1% HCOOH over 10 min. Preparative HPLC was performed using a UltiMate 3000, equipped with a Gemini-NX C18 110 Å column (Phenomenex) running at a flow rate of 10.0 ml/min and a linear gradient going from 95% H₂O/5% acetonitrile with 0.1% TFA to 100% acetonitrile with 0.1% TFA over 30 min. High-resolution mass spectra were obtained on a Micromass LCT high-resolution time-of-flight instrument by direct injection. Ionization was performed in positive electrospray mode.

General Methods for Solid-Phase Peptide Synthesis. Peptide synthesis was performed using *N* $^{\alpha}$ -Fmoc-protected amino acids and a HBTU/HOBt activation protocol using a TentaGel resin with Rink amide linker (0.23 mmol/g), HBTU (3.8 Eq), HOBt/HOAt (4:1, 4 Eq), Fmoc-protected amino acids (4 Eq), and DIPEA (7.2 Eq) in NMP. Preactivation was for 5 min, and single couplings were for 90 min. Fmoc deprotection was performed using piperidine-NMP (1:4) for 2 + 15 min. Peptides with Alloc-protected amino acids were deprotected to a free amine by treating the fully protected and *N*-acetylated peptides with a mixture of Pd(PPh₃)₄ (0.05 Eq) and Me₂NH · BH₃ (0.2 Eq) in degassed CH₂Cl₂ (30 min) and washed with NMP (5 \times). The peptides were then treated with *N*, *N'*-di-Boc-1*H*-pyrazole-1-carboxamide (5 Eq) in NMP overnight. After peptide assembly, the resins were washed extensively with NMP and CH₂Cl₂, before peptide release with TFA-H₂O-triethylsilane (95:2.5:2.5). Peptide release normally proceeded for 2 h before the TFA-peptide mixture was collected by filtration. The resin was additionally washed with TFA (two times), and the TFA mixtures were pooled. TFA was removed under a stream of nitrogen, and the peptide was precipitated with diethyl ether. The synthesized peptides were dissolved in a minimum amount of H₂O-acetonitrile (2:1) before being purified by preparative HPLC. The purified peptides were dissolved in H₂O-acetonitrile (2:1) to a final concentration of 1 mM. The solution was brought to pH 7.5 to 8 with NH₃ in methanol. The

peptides were oxidized to form disulfide bridges, either by addition of 1.2 Eq of H_2O_2 (30–60 min) or by bubbling atmospheric air through the solution (1–3 days). The use of H_2O_2 is only applicable in peptides without a methionine (upain-2 and mupain-1 variants). The oxidation was stopped with the addition of acetic acid (0.1 ml) followed by evaporation and HPLC purification.

Synthesis of Fmoc-Dap(4-(2,3-bis(Boc)guanidino)benzoate)-OH (Protected Form of 11). Benzotriazol-1-yloxy-tripyrrolidinophosphonium hexafluorophosphate (1040 mg, 2.0 mmol) and DIPEA (0.35 ml, 2.0 mmol) were added to a solution of 4-(2,3-bis(*tert*-butoxycarbonyl)guanidino)benzoic acid (800 mg, 2.1 mmol) in CH_2Cl_2 (5 ml). The mixture was stirred for 10 min at room temperature and transferred to a solution of Fmoc-Dap-OH (326 mg, 1.0 mmol) in CH_2Cl_2 (6 ml). DIPEA (0.35 ml, 2.0 mmol) was added, and the mixture was stirred for 18 h at room temperature. The mixture was evaporated and purified by column chromatography with ethyl acetate-acetic acid (99:1) to afford the product as a yellow oil (421 mg, 61%). ^1H NMR (300 MHz, CDCl_3) δ ppm 7.78–7.48 (m, 10H), 7.38–7.20 (m, 4H), 4.45–4.05 (m, 3H), 3.88–3.63 (m, 2H), 1.50–1.62 (bs, 9H). ^{13}C (75 MHz, CDCl_3) δ ppm 172.2, 168.6, 156.9, 153.6, 143.7, 143.6, 141.2, 141.1, 139.8, 129.4, 128.7, 128.2, 127.6, 127.0, 125.1, 122.2, 120.9, 119.8, 67.3, 55.1, 46.9, 28.0. HRMS (ES) exact mass calculated for $\text{C}_{26}\text{H}_{26}\text{N}_5\text{O}_5$ ($\text{M} + \text{H} - 2\text{Boc}$), 488.1934. Found, 488.1938.

Synthesis of Fmoc-4-(*N,N'*-di-Cbz-guanidine)-cyclohexylalanine-OH (Protected Form of 15). To a degassed (argon) solution of Boc-Phe(4- NO_2)-OH (1 g, 3.22 mmol) in acetic acid (3 ml) and methanol (3 ml) was added PtO_2 (500 mg), and H_2 was bubbled through the mixture until completion of the reaction as determined by HPLC (9 h). The mixture was coevaporated several times with toluene. The green solid was dissolved in dimethylformamide (5 ml), and to this mixture was added *N,N'*-bis(benzyloxycarbonyl)-1*H*-pyrazole-1-carboxamide (1250 mg, 3.30 mmol) and Et_3N (0.45 ml, 3.23 mmol) and left stirring overnight. The mixture was evaporated, and ethyl acetate (30 ml) was added and extracted with aqueous NaHCO_3 (10%, three 20-ml extractions). The aqueous solution was acidified to pH 2 to 3 with aqueous HCl (37%) and extracted with CH_2Cl_2 (three 30-ml extractions) and evaporated. $\text{TFA-CH}_2\text{Cl}_2$ (1:1, 10 ml) was added, and the mixture was stirred for 15 min and then evaporated to an oil and left on high vacuum overnight. The solid was dissolved in $\text{H}_2\text{O-dioxane}$ (1:2, 60 ml). To this was added Fmoc-OSu (1.20 g, 3.56 mmol) and NaHCO_3 (550 mg, 6.55 mmol), and the mixture was left stirring overnight. The mixture was evaporated and redissolved in acetic acid (5 ml), and celite (3 g) was added. The slurry was evaporated and purified by silica gel column chromatography with ethyl acetate-heptane-acetic acid (50:50:1) providing 813 mg (35%). The product is presumably a *cis/trans* isomer (Rao et al., 1991). ^1H NMR (300 MHz, CDCl_3) δ ppm 7.55 to 7.63 (d, $J = 7.3$ Hz, 2H), 7.52 to 7.61 (m, 2H), 7.32 to 7.45 (m, 10H), 5.16 to 5.05 (m, 5H), 4.31 to 4.05 (m, 4H), 2.59 (s, 0.2H), 2.30 (s, 0.8H), 2.05 to 1.02 (m, 8H). ^{13}C (75 MHz, CDCl_3) δ ppm 176.6, 176.5, 163.8, 156.1, 155.2, 155.1, 154.0, 153.8, 148.5, 143.9, 143.8, 143.6, 141.3, 137.8, 136.8, 136.8, 134.6, 134.5, 134.5, 125.0, 120.0, 68.4, 68.1, 67.1, 51.7, 49.5, 47.1, 46.3, 38.6, 32.4, 32.2, 30.5, 29.2, 29.1, 28.1, 26.9, 21.4. HRMS (ES) exact mass calculated for $\text{C}_{41}\text{H}_{43}\text{N}_4\text{O}_8$ ($\text{M} + \text{H}$): 719.3081. Found: 719.3044.

Synthesis of Fmoc-L-3-(*N*-amidino-3-piperidyl)alanine-OH (Precursor for 17). Fmoc-L-3Pal-OH (700 mg, 1.8 mmol) was dissolved in acetic acid (10 ml) in a round-bottomed flask, and PtO_2 (500 mg) was added. The solution was degassed, the flask was connected to a hydrogen balloon, and the mixture was left stirring overnight. The mixture was filtered and evaporated to a clear oil. The oil was further evaporated with toluene (three 30-ml washes) to remove acetic acid residues. The oil was dissolved in acetonitrile- H_2O (2:1, 50 ml) and DIPEA (0.15 ml, 0.9 mmol), and Alloc $_2\text{O}$ (285 mg, 2.0 mmol) was added. The mixture was stirred at room temperature until the completion of the reaction as determined by HPLC (1 h). The mixture was evaporated and purified by column chromatography with ethyl acetate-heptane-acetic acid (1:1:0.02) to afford the product as a white foam (650 mg, 75%). The product is presumably a mixture of diaste-

reomers (Hartung et al., 2005). ^1H (300 MHz, CDCl_3) δ ppm 8.02 (s, 1H), 7.76 (d, $J = 7.5$ Hz, 1H), 7.60 (d, $J = 6.3$ Hz, 1H), 7.40 (t, $J = 7.3$ Hz, 1H), 7.35 to 7.24 (m, 1H), 5.93 (dd, $J = 16.3$, 9.6 Hz, 1H), 5.34 to 5.03 (m, 1H), 4.71 to 4.32 (m, 3H), 4.23 (t, $J = 7.0$ Hz, 1H), 4.03 to 3.75 (m, 1H), 3.12 to 2.46 (m, 1H), 1.97 to 1.04 (m, 4H). ^{13}C (75 MHz, CDCl_3) δ ppm 176.09, 156.52, 156.24, 155.50, 143.95, 143.74, 141.37, 133.00, 127.80, 127.16, 126.13, 125.22, 120.06, 117.60, 116.49, 67.63, 67.20, 66.38, 51.89, 51.64, 49.78, 49.03, 47.20, 44.72, 36.04, 32.41, 30.62, 29.87, 24.43. MS (ES) calculated for $\text{C}_{27}\text{H}_{31}\text{N}_2\text{O}_6$ ($\text{M} + \text{H}$), 479.2. Found, 479.1.

Synthesis of Fmoc-3-(*N,N'*-di-Boc-guanidine)-Tyr-OH (Protected Form of 14). A solution of H-Tyr(3- NO_2)-OH (1000 mg, 4.42 mmol) in dioxane- H_2O (2:1, 20 ml), NaHCO_3 (1280 mg, 15.2 mmol), and Fmoc-OSu (1710 mg, 5.1 mmol) in a round-bottomed flask was stirred overnight at room temperature. After the solution was degassed, Pd/C was added, and a hydrogen balloon was connected. The mixture was stirred for 2 h, filtered (celite), and evaporated. To this solid was added CH_2Cl_2 (5 ml), which formed a suspension, and *N,N'*-di-Boc-1*H*-pyrazole-1-carboxamide (1530 mg, 4.94 mmol) was added and the mixture was left stirring overnight. The mixture was evaporated with celite and purified by column chromatography with ethyl acetate-heptane-acetic acid (1:1:0.01) providing 1980 mg (68%). ^1H NMR (300 MHz, CDCl_3) δ ppm 10.1 (bs, 4H), 7.82 to 7.13 (m, 11H), 7.04 to 6.77 (m, 3H), 5.48 (d, $J = 7.7$ Hz, 1H), 4.53 to 4.12 (m, 4H), 3.32 to 2.95 (m, 2H), 1.61 to 1.40 (bs, 18H). ^{13}C (75 MHz, CDCl_3) δ ppm 174.9, 160.9, 155.8, 153.1, 153.0, 148.4, 143.8, 143.7, 141.3, 141.2, 132.9, 129.0, 128.7, 128.2, 127.7, 127.1, 125.3, 125.2, 125.1, 124.7, 124.6, 121.0, 119.9, 84.7, 80.9, 67.1, 54.9, 47.1, 36.7, 28.1, 21.4. HRMS (ES) exact mass calculated for $\text{C}_{25}\text{H}_{25}\text{N}_4\text{O}_5$ ($\text{M} + \text{H} - 2\text{Boc}$), 461.1825. Found, 461.1831.

Synthesis of Fmoc-L-phenylglycine-3-(*N,N'*-di-Boc-guanidine)-OH (Protected Form of 13). L-Phenylglycine (5 g, 33 mmol) was dissolved in 97% H_2SO_4 (12 ml) and cooled to 0°C. To this solution was added 37% HNO_3 (1.5 ml, 36 mmol) dropwise. The mixture was stirred at 0°C for 1 h and neutralized with 25% $\text{NH}_4\text{OH}/\text{H}_2\text{O}$ (20 ml). When the mixture reached pH 7, a yellow precipitate formed, which was filtered off and washed with ice-cold deionized H_2O . The precipitate was recrystallized with H_2O to afford 3-nitrophenylglycine as a white solid (Sassatelli et al., 2006). The solids were dissolved in $\text{H}_2\text{O-dioxane}$ (2:3, 100 ml). Fmoc-OSu (7.0 g, 21 mmol) and Na_2CO_3 (3.6 g, 34 mmol) were added. The mixture was stirred at room temperature (18 h) and acidified to pH 2 by 37% HCl . To this was added H_2O (150 ml), and the mixture was extracted with ethyl acetate (100 ml). The organic phase was washed with H_2O (100 ml) and brine (100 ml) and evaporated. Acetic acid (50 ml) and Pd/C (300 mg) was added, and the mixture was left stirring under 1 atm H_2 for 12 h. The mixture was filtered with celite and evaporated to a yellow oil (8.72 g). To 450 mg of this oil in dimethylformamide (10 ml) was added *N,N'*-di-Boc-1*H*-pyrazole-1-carboxamide (400 mg, 1.3 mmol) and triethylamine (0.35 ml, 2.5 mmol), and the mixture was stirred for 3 h at room temperature. The mixture was evaporated and purified by column chromatography with heptane-ethyl acetate-acetic acid (40:40:1) to give the product (620 mg, 85%) as a yellow foam. ^1H NMR (300 MHz, CDCl_3) δ ppm 1.34 to 1.63 (m, 18H) 4.07 to 4.55 (m, 3H) 4.94 to 5.42 (m, 1H) 6.00 to 6.43 (m, 1H) 7.03 to 8.10 (m, 15H). ^{13}C (75 MHz, CDCl_3) δ ppm 28.1, 31.2, 47.2, 58.0, 67.2, 105.6, 119.9, 122.1, 123.3, 123.7, 124.3, 125.2, 127.1, 127.7, 128.3, 129.1, 129.5, 133.0, 136.5, 137.9, 138.3, 141.3, 143.9, 153.2, 154.2, 155.5, 160.4, 173.1. HRMS (ES) exact mass calculated for $\text{C}_{34}\text{H}_{39}\text{N}_4\text{O}_8$, 631.2768. Found, 631.2767.

Synthesis of (S)-2-Acetamido-6-guanidinohexanamide. To a solution of Fmoc-Lys(Alloc)-OH (181 mg, 0.4 mmol) in NMP (2 ml) was added HBTU (140 mg, 0.37 mmol) and DIPEA (0.12 ml, 0.72 mmol), and the mixture was added to TentaGel resin (417 mg, 0.1 mmol). The mixture was carefully shaken (2 h) and washed several times with NMP. The resin was treated with piperidine-NMP (1:4, 2 + 15 min), washed several times with NMP and CH_2Cl_2 , and treated with $\text{Ac}_2\text{O-CH}_2\text{Cl}_2$ (1:2, two 7-min treatments). To the resin

was added degassed CH_2Cl_2 and $\text{Pd}(\text{PPh}_3)_4$ (30 mg, 0.026 mmol) and $\text{BH}_3 \cdot \text{HN}(\text{CH}_3)_2$ complex (25 mg, 0.45 mmol). The mixture was shaken for 30 min and washed several times with NMP. To the resin was added N,N' -di-Boc-1H-pyrazole-1-carboxamide (310 mg, 1.0 mmol) in NMP (2 ml), and the mixture was shaken overnight at room temperature. The resin was treated with TFA-triethylsilane- H_2O (95:2.5:2.5, 2 h). The mixture was evaporated under a stream of N_2 , and the product was purified by preparative HPLC to provide 14 mg (64%). ^1H NMR (300 MHz, D_2O) δ 4.25 (dd, J = 8.9, 5.4 Hz, 1H), 3.20 (t, J = 6.9 Hz, 2H), 1.92 to 1.69 (m, 2H), 1.61 (dd, J = 14.4, 6.9 Hz, 2H), 1.52 to 1.35 (m, 2H). ^{13}C NMR (75 MHz, D_2O) δ ppm 156.7, 53.4, 40.8, 30.4, 27.3, 22.1, 21.6. HRMS (ES) exact mass calculated for $\text{C}_9\text{H}_{20}\text{N}_5\text{O}_2$ (M + H), 230.1617. Found, 230.1609.

Synthesis of (S)-2-Acetamido-3-(4-guanidinophenyl)propanamide. HBTU (140 mg, 0.37 mmol) and DIPEA (0.12 ml, 0.72 mmol) were added to a solution of Fmoc-4-guanidino-phenylalanine(N,N' -di-Boc)-OH (258 mg, 0.4 mmol) in NMP (2 ml), and the mixture was added to Tentagel resin (417 mg, 0.1 mmol). The mixture was carefully shaken (2 h) and washed several times with NMP. To the resin was added piperidine-NMP (1:4, 2 + 15 min), and the mixture was washed several times with NMP and CH_2Cl_2 . Subsequently the resin was treated with $\text{Ac}_2\text{O}-\text{CH}_2\text{Cl}_2$ (1:2, two 7-min treatments) and washed several times with CH_2Cl_2 . The resin was then treated with TFA-triethylsilane- H_2O (95:2.5:2.5, 2 h). The mixture was evaporated under a N_2 flow, and the product was purified by preparative HPLC (11 mg, 44%). ^1H NMR (300 MHz, D_2O) δ 7.57 to 7.25 (m, 4H), 4.66 to 4.54 (m, 1H), 3.25 (dd, J = 14.0, 6.0 Hz, 1H), 3.03 (dd, J = 13.9, 9.3 Hz, 1H), 1.96 (s, 3H). ^{13}C NMR (75 MHz, D_2O) δ 137.5, 136.1, 132.5, 130.3, 130.1, 128.2, 125.5, 122.6, 118.7, 118.2, 117.8, 114.0, 54.1, 36.1, 21.1. HRMS (ES) exact mass calculated for $\text{C}_{12}\text{H}_{18}\text{N}_5\text{O}_2$ (M + H), 264.1461. Found, 264.1476.

Synthesis of (S)-2-Acetamido-3-(1-carbamimidoylpiperidin-4-yl)propanamide. To a solution of Fmoc-L-Ala(4-Pip(Alloc))-OH (191 mg, 0.4 mmol) in NMP (2 ml) was added HBTU (140 mg, 0.37 mmol) and DIPEA (0.12 ml, 0.72 mmol), and the mixture was added to a Tentagel resin (417 mg, 0.1 mmol). The mixture was carefully shaken (2 h) and washed several times with NMP. The resin was treated with piperidine-NMP (1:4, 2 + 15 min), and the mixture washed several times with NMP and CH_2Cl_2 . Then the resin was treated with $\text{Ac}_2\text{O}-\text{CH}_2\text{Cl}_2$ (1:2, two 7-min treatments) and washed several times with CH_2Cl_2 . To the resin was added degassed CH_2Cl_2 , $\text{BH}_3 \cdot \text{HN}(\text{CH}_3)_2$ complex (25 mg, 0.45 mmol), and $\text{Pd}(\text{PPh}_3)_4$ (30 mg, 0.026 mmol). The mixture was shaken for 30 min and washed several times with NMP. N,N' -Di-Boc-1H-pyrazole-1-carboxamide (310 mg, 1.0 mmol) in NMP (2 ml) was added, and the mixture was shaken overnight at room temperature. The resin was treated with TFA-triethylsilane- H_2O (95:2.5:2.5, 2 h). The mixture was evaporated under a N_2 flow, and the product was purified by preparative HPLC (10 mg, 39%). ^1H NMR (300 MHz, D_2O) δ 4.22 (t, J = 7.3 Hz, 1H), 3.70 (d, J = 13.8 Hz, 2H), 2.95 (dd, J = 23.7, 10.9 Hz, 2H), 1.94 (s, 3H), 1.76 to 1.52 (m, 5H), 1.29 to 1.02 (m, 2H). ^{13}C NMR (75 MHz, D_2O) δ ppm 177.3, 174.4, 155.6, 51.1, 45.8, 45.7, 37.0, 31.4, 30.9, 29.7, 21.6. HRMS (ES) exact mass calculated for $\text{C}_{11}\text{H}_{22}\text{N}_5\text{O}_2$ (M + H), 256.1774. Found, 256.1782.

Recombinant uPA Expression and Purification. Two-chain human uPA, originating from urine, was purchased from Wakamoto Pharmaceutical Company (Tokyo, Japan) or Prospe (Rehovot, Israel). Human uPA concentrations were determined from the absorbance at 280 nm, using an extinction coefficient of $1.36 \text{ ml} \cdot \text{mg}^{-1} \cdot \text{cm}^{-1}$ and M_r of 54,000. Two-chain murine uPA was purchased from Molecular Innovations (Novi, MI). Wild-type and mutant recombinant human and murine uPA were expressed in and in some cases purified from human embryonic kidney 293T cells transfected with the corresponding cDNAs in pcDNA3.1 (Petersen et al., 2001; Andersen et al., 2008).

When the cells were cultured without addition of protease inhibitors able to inhibit the conversion of single-chain pro-uPA to active two-chain uPA, such as aprotinin, approximately 50% of the uPA in the conditioned medium and the purified preparations was in the

active form and could thus be used directly for enzymatic assays. Three sets of mutant cDNAs were cloned into pcDNA3.1 and used to obtain the corresponding proteins. First, murinized human uPA variants, harboring the point mutations H99Y,² Q192K, or H99Y-Q192K, were those described previously (Andersen et al., 2008). Second, humanized murine uPA variants, in which the point mutation K192Q was introduced into murine uPA or in which the human 37, 60, and 99 loops were grafted onto murine uPA, were constructed by standard cloning procedures and customized DNA synthesis (GenScript, Piscataway, NJ). More specifically, the murine uPA variant with human 37, 60, and 99 loops harbors the mutations Q35R, K36R, N37H, K37aR, Q60aD, L60bY, N63D, and Y99H. Third, cDNA corresponding to chimeras of human and mouse uPA, in which positions 22 to 120 or 121 to 250 of human uPA replaced the corresponding residues in a murine uPA background, were synthesized by GenScript. Conditioned media from the HEK293T transfectants were used directly for the analysis of kinetic parameters and inhibition constants for the various uPA variants. In a few cases (wt human uPA, wt murine uPA, murine uPA with human residues 16 to 120, and murine uPA with human residues 121 to 250), it was shown that the same kinetic parameters and inhibition constants were obtained with conditioned media and purified preparations.

The cloning strategy and the production of the recombinant uPA catalytic domain (residues 159–411) to be used for crystallization were described previously (Zhao et al., 2007). In brief, the recombinant uPA catalytic domain was secreted from a stable *Pichia pastoris* strain (X-33) after induction by methanol and captured by a cation exchange column. The protein was further purified on a gel filtration column (Superdex 75 HR 10/30 column; GE Healthcare, Chalfont St. Giles, Buckinghamshire, UK) equilibrated with 20 mM sodium phosphate, pH 6.5, 150 mM NaCl. The protein was eluted as a single peak under these conditions, with a retention time of approximately 13.6 ml. The recombinant uPA catalytic domain expressed this way is an active protease with an activity comparable with that of full-length two-chain uPA (Zhao et al., 2007). The protein was dialyzed in 20 mM potassium phosphate, pH 6.5, overnight and concentrated to 10 mg/ml, using stirred ultrafiltration cells (Millipore Amicon Bioseparations, model 5124; Thermo Fisher Scientific, Waltham, MA) before protein crystallization.

Determination of K_M Values for uPA-Catalyzed Hydrolysis of S-2444. To determine the K_M and maximal velocity (V_{max}) values for the uPA-catalyzed hydrolysis of the chromogenic substrate S-2444, a 200- μl 2-fold dilution series of the substrate S-2444 (0–4 mM) in a buffer of 10 mM HEPES, pH 7.4, 140 mM NaCl (HEPES-buffered saline), with 0.1% bovine serum albumin, was incubated 2 min at 37°C before the addition of a fixed concentration of uPA (4 nM final concentration). The initial reaction velocities (V_i), monitored as the changes in absorbance at 405 nm, were plotted against the initial substrate concentration ($[S]$) and nonlinear regression analysis was used to determine the K_M according to eq. 1:

$$V_i = V_{\text{max}}[S]/([S] + K_M) \quad (1)$$

The K_M values for all the uPA variants used in the present study are listed in Supplemental Table 1.

Determination of K_i Values for the Inhibition of uPA Variants by Upain-2 and Mupain-1 Variants. The concentrations of the peptide variants were determined by measurements of OD_{280} and the use of sequence-derived extinction coefficients provided by the ProtParam tool provided by the Expasy server (located at <http://www.expasy.org>). For routine determination of K_i values for the inhibition of the various uPA variants under steady-state inhibition conditions, a fixed concentration of purified uPA or uPA-containing conditioned media from transfected cells (2 nM uPA as the final concentration) was preincubated in 200 μl of HEPES-buffered saline

² Amino acid numbering used in the text and figures refers to the standard chymotrypsinogen template numbering.

with 0.1% bovine serum albumin at 37°C, with various concentrations of upain-2 or mupain-1 variant peptides (0–400 μM) for 15 min before the addition of the chromogenic substrate S-2444 in concentrations approximately equal to the K_M value for each particular variant. The initial reaction velocities were monitored at an absorbance of 405 nm. The inhibition constants (K_i) were subsequently determined from the nonlinear regression analyses of plots for V_i/V_0 versus $[I]_0$ using eq. 2, derived under an assumption of competitive inhibition:

$$V_i/V_0 = (K_i \times (K_M + [S]_0)) / ((K_i \times [S]_0) + (K_M \times (K_i + [I]_0))) \quad (2)$$

where V_i and V_0 are the reaction velocities in the presence and absence of inhibitor, respectively; $[S]_0$ and $[I]_0$ are the substrate and inhibitor concentrations, respectively, and K_M is the K_M for the uPA catalyzed hydrolysis of S-2444. In eq. 2, it is assumed that $[S]_{\text{free}} \approx [S]_0$ and $[I]_{\text{free}} \approx [I]_0$. These conditions were fulfilled because less than 10% of the substrate was converted to product in the assays and because the assay typically contained a final concentration of uPA variant of 2 nM and inhibitor concentrations in the micromolar range.

In cases for which we observed no measurable inhibition (i.e., <10%) at 400 μM , the maximal inhibitor concentration used, the accuracy of the assay allowed us to conclude that the K_i value was above 1000 μM (indicated as ">1000 μM " in the tables). In other cases in which we did observe a measurable inhibition at 400 μM , we were still unable to accurately determine K_i values more than 500 μM (indicated as ">500 μM " in the tables).

The validity of performing the K_i determinations with uPA-containing conditioned media from transfected cells was verified by controls in which the determinations were performed with conditioned media as well as with purified preparations. These controls were performed with wt murine uPA, wt human uPA, human uPA Q192K, murine uPA, and human residues 16 to 120, obtaining indistinguishable values with the types of samples.

X-Ray Crystal Structure Analysis. The crystallization trials were performed using the method of sitting drop vapor diffusion. The crystals of the uPA catalytic domain were obtained by equilibrating against a reservoir solution containing 2.0 M ammonium sulfate, 50 mM sodium citrate, pH 4.6, and 5% PEG 400 at room temperature. The crystals appeared in approximately 3 days. For the uPA-upain-2-13 complex, the crystals of uPA were then soaked for 2 weeks in crystallization mother liquid containing 1 mM upain-2-13. Before X-ray data collection, the crystals were soaked for 5 min in a cryoprotectant solution (2.0 M ammonium sulfate, 5% polyethylene glycol 400, 100 mM Tris-HCl, pH 7.4, and 20% glycerol).

X-ray diffraction data for the crystals were collected at the BL17U1 beamline (Shanghai Synchrotron Radiation Facility, Shanghai, China). All diffraction data were indexed and integrated with the HKL2000 program package (Otwinowski and Minor, 1997).

The crystal structure of the uPA-upain-2-13 complex was solved by molecular replacement with the CCP4 program package (Collaborative Computational Project, Number 4, 1994), using the structure of the uPA catalytic domain (PDB file 2NWN) (Zhao et al., 2007) as the search model. The electron density for the peptide was clearly visible in the uPA active site and was modeled on the basis of the $F_o - F_c$ difference map. The structure was refined with the CCP4 program package and manually adjusted with the molecular graphics program Coot (Emsley and Cowtan, 2004) iteratively until the convergence of the refinement. Solvent molecules were added using a $F_o - F_c$ Fourier difference map at 2.5 σ in the final refinement step. The final structures were analyzed by software PyMOL (DeLano, 2002).

Results

Non-Natural Arginine Analogs. The P1 Arg residue in mupain-1 was systematically substituted with a series of Arg

analogs. Concerning upain-1, the novel P1 residues were substituted into the modified sequence CSWRGLENHAAAC (upain-2).³ This modification was chosen because the cyclization step could be performed much faster when Arg10 of upain-1 (CSWRGLENHRMC) was replaced with Ala and, secondly, H_2O_2 could be used as an oxidant when Met11 was absent. As predicted from our previous report (Hansen et al., 2005), the modified sequence bound to human uPA with a K_i indistinguishable from that of the original peptide: $35 \pm 8 \mu\text{M}$ ($n = 5$) for the modified sequence versus $30 \pm 1 \mu\text{M}$ ($n = 3$) for the original sequence. When planning which arginine analogs to test as the P1 residue in upain-2 and mupain-1, we considered varying several parameters, all expected to affect the interaction of the P1 residue with the S1 pocket (Table 1).

1. The chirality of the P1 residue was tested by substituting L-Arg (1) with D-Arg (3).
2. The length of the aliphatic side chain was tested by substituting arginine with homologs containing one to five methylene groups between the α -carbon and the guanidino group (4–7). Besides determining how far the guanidino moiety can insert into the S1 pocket, the spacer length could also have an effect on the binding entropy and the strength of hydrophobic interactions.
3. The exact nature of the basic group could be tested by replacing the guanidino group of L-Arg with a urea moiety ($\text{p}K_a = 12$), an amino group ($\text{p}K_a = 10$), or a guanidino-oxo group ($\text{p}K_a = 7$) (Boyar and Marsh, 1982).
4. The structure of the carbon skeleton between the α -carbon and the basic group was varied by introducing aliphatic or aromatic rings (11–14). Aromatic rings would be spatially more demanding and restrict the conformational orientations and potentially mimic already reported small molecule inhibitors. They would also result in a lower $\text{p}K_a$ value for the guanidino moiety. Cyclic aliphatic groups would restrict the conformational orientations (15–17).

Although a variety of arginine analogs are commercially available, more arginine analogs had to be synthesized de novo (Fig. 1) to complete the planned scan of the P1 position (Table 1). We here designed and synthesized the following novel arginine analogs: 4-guanidino-L-cyclohexylalanine (15), 3-guanidino-L-tyrosine (14), 3-guanidino-L-phenylglycine (13), (S)-2-amino-3-(4-guanidinobenzamido)propanoic acid (11), and L-3-(N-amidino-3-piperidyl)alanine (17).

With the de novo synthesized arginine analogs and the commercially available analogs at hand for insertion into the P1 position, linear forms of the peptides were assembled by solid-phase peptide synthesis. The peptides were obtained as the N-terminal acetylated and C-terminal amidated forms and were cyclized by disulfide bridge formation.

Effects of P1 Substitutions on the Inhibition of Human uPA by Upain-2 and of Murine uPA by Mupain-1. We investigated the effect of substituting the different analogs into the P1 position of upain-2 or mupain-1 on their ability to inhibit human or murine uPA (Table 1). The binding of the peptide to their targets was critically dependent on the side chain of the P1 residue, because substitution of P1 Arg with Ala (2) abolished all inhibitory activity.

³ Each of the amino acids tested as the P1 residue was given a number n between 1 and 19 (Table 1). The corresponding variants of upain-2 and mupain-1 were named upain-2- n and mupain-1- n , respectively.

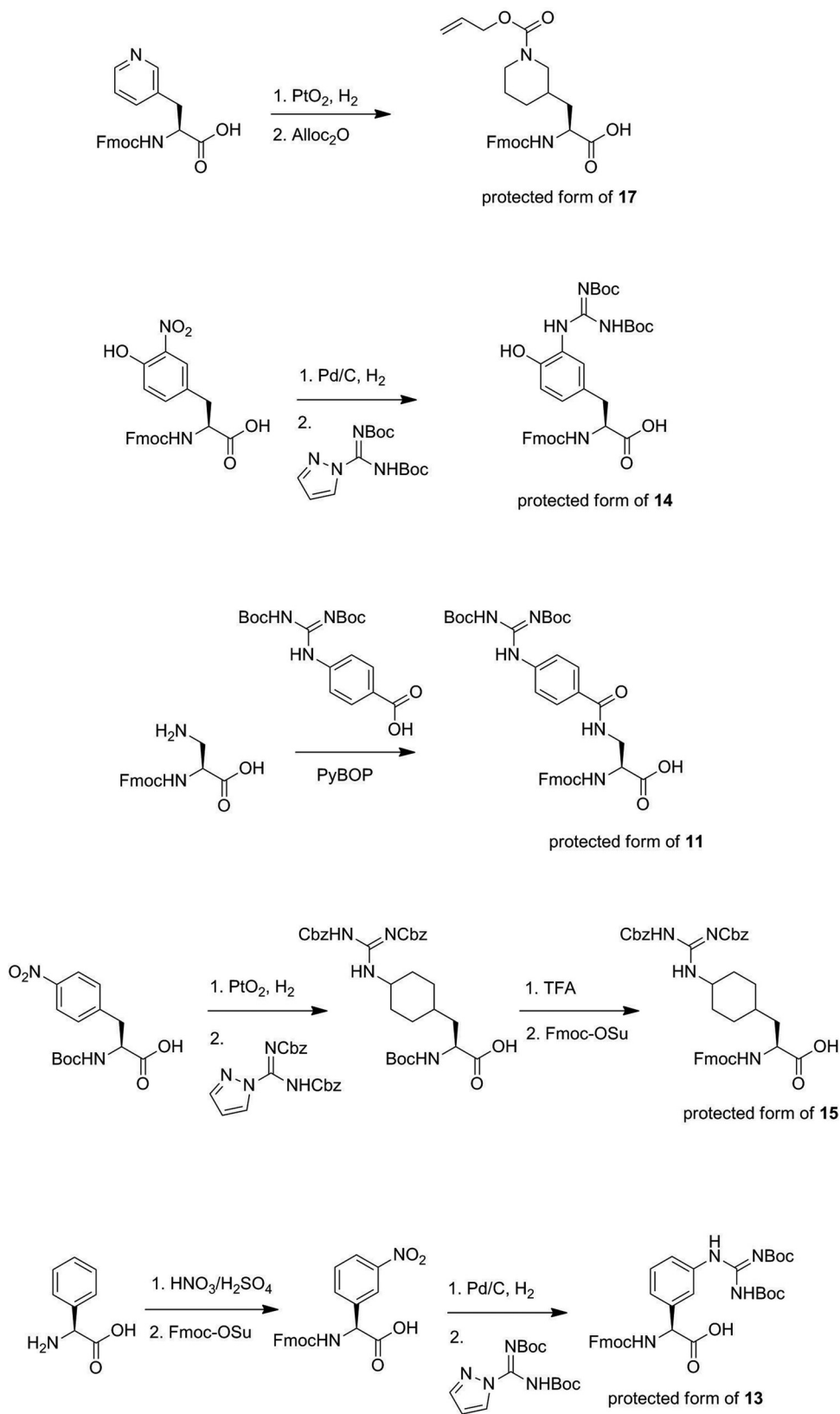


Fig. 1. Synthesis of novel arginine analogs for use as P1 residues in upain-2 and mupain-1. Chemical synthesis of the protected forms of new Arg analogs **11**, **13**, **14**, and **15** as well as the protected form of the precursor for **17**. After incorporation of **17** into peptides, the Alloc protection was removed and the liberated amine guanidylated on-resin. Similar chemical processes were used for the construction of peptides containing homoarginine.

Substitution of P1 Arg in upain-2 with a number of L-Arg analogs with linear aliphatic side chains (**3–10**) in almost all cases resulted in a strong loss of activity. Neither a change in chirality, variation in the chain length, nor exchange of the guanidino group with a urea moiety, an amino group, or a guanidino-oxo group was accepted. The only exception was substitution with L-homo-arginine (**6**), which resulted in a slight improvement of affinity. Moreover, substitution with aromatic (**11–14**) or aliphatic ring structures (**15–17**) always resulted in a strong loss of inhibitory activity.

Similar to upain-2, substitution of the P1 Arg in mupain-1 with L-Arg analogs containing linear aliphatic side chains (**3–10**) in all cases resulted in loss of inhibitory activity, with an increase in K_i of between 5 and >2000-fold. The response to substitution with L-Arg analogs with aromatic ring structures (**11–14**) was more varied, because the substitution with the Phe analog **12** resulted in a slight increase in affinity, whereas other substitutions resulted in a strong loss of affinity. Moreover, inhibition of murine uPA could still be achieved with L-Arg analogs with aliphatic ring structures (**15–17**). In fact, substitution with the amidino compound **16** resulted in a 10-fold increase in affinity (Table 1). Thus, in contrast to upain-2, with mupain-1 we managed to achieve a considerable increase in affinity to the target enzyme by suitable substitutions.

The effects of substituting the same amino acid into the P1 position was in several cases strikingly different for upain-2 targeting human uPA compared with mupain-1 targeting murine uPA. Substitution with L-homo-arginine (**6**) increased the affinity of upain-2 to human uPA but decreased the affinity of mupain-1 to murine uPA 5-fold; substitution with the Phe derivative **12** or the amidino compound **16**, respectively, decreased the affinity of upain-2 to human uPA, but increased the affinity of mupain-1 to murine uPA.

We confirmed the competitive nature of the inhibition with selected peptides (i.e., mupain-1-**12** and mupain-1-**16**). The K_i values determined for inhibition of murine uPA, calculated with eq. 2, were found to be indistinguishable at substrate concentrations ranging from 0.2 to 3 times the K_m value.

An important finding was that the amidino compound **16**, L-homo-arginine (**6**), and the Phe derivative **12**, as free N-terminal acetylated and C-terminal amidated amino acids, were unable to inhibit human or murine uPA measurably in concentrations up to 400 μ M (data not shown).

Effects of P1 Substitutions on the Inhibition of Chimeras between Human and Murine uPA by Mupain-1 and Upain-2. We considered two different hypotheses for the different effects of P1 substitutions on upain-2 inhibition of human uPA and on mupain-1 inhibition of murine uPA:

1. The different responses to the substitutions in human uPA on one side and murine uPA on the other could be due to the new amino acids in the P1 positions fitting differently into the S1 pockets of human and murine uPA, respectively.
2. The different responses to the P1 substitutions on inhibition of human and murine uPA could be related to the fact that the effect of a certain P1 substitution is strongly affected by the exosite interactions. As expected from the different sequences of the two peptides outside the P1 position and as demonstrated by site-directed mutagenesis

and X-ray crystal structure determination (Hansen et al., 2005; Zhao et al., 2007; Andersen et al., 2008), the exosite interactions are very different for upain-2 and mupain-1. The exosite interactions may restrict the way the P1 residue inserts into the S1 pocket and vice versa, thus determining how a certain P1 substitution affects the affinity.

To distinguish between these two possibilities, we constructed chimeras in which exosite and S1 pocket residues were exchanged between human and murine uPA. The choice of exosites was based on previous results from site-directed mutagenesis and X-ray crystal structure analysis (Fig. 2). We previously demonstrated that “murinization” of human uPA in position 99 (i.e., generation of human uPA H99Y) made human uPA sensitive to inhibition by mupain-1, however with a K_i value approximately 20-fold higher than the K_i value for inhibition of murine uPA (Andersen et al., 2008). We therefore used human uPA H99Y to study the importance of exosite interactions for mupain-1 binding. We also previously demonstrated the importance of the so-called 37 and 60 loops and of position 99 of human uPA for binding of upain-1 (Hansen et al., 2005; Zhao et al., 2007) (Fig. 2). We now constructed and expressed a “humanized” murine uPA, with a human 37-loop (murine uPA Q35R, K36R, N37H, and K37aR), a human 60-loop (murine uPA Q60aD, L60bY, and N63D), and the human 99-residue grafted onto murine uPA (murine uPA Y99H). To evaluate the contribution from the S1 pocket, we constructed a human uPA variant that was murinized in position 192 (human uPA Q192K) and a variant of murine uPA that was humanized in position 192 (murine uPA K192Q). Position 192 is the only position with a nonconserved amino acid among the positions with residues lining the S1 pocket (Fig. 2).

As a more radical way of exchanging residues, we constructed variants of murine uPA in which either the N-terminal β -barrel (residues 16–120) or the C-terminal β -barrel (residues 120–250) of the catalytic domain was replaced by the corresponding sequences of human uPA. All identified exosite interactions between upain-1 and human uPA involving nonconserved residues are present in the N-terminal β -barrel. Likewise, all identified exosite interactions between upain-1 and human uPA involving nonconserved residues are present in this β -barrel. In contrast, the S1 pocket is totally embedded in the C-terminal β -barrel (Fig. 2).

We then tested the susceptibility of the constructed chimeras to the original upain-2 and mupain-1 peptides and to selected P1-substituted variants of upain-2 and mupain-1. The variants selected were variants with the amidino compound **16**, L-homo-arginine (**6**), or the Phe derivative **12** as the P1 residue, because of the differential effect these substitutions have on the affinity of upain-2 to human uPA and of mupain-1 to murine uPA (Table 2).

By inspecting the data, it is seen that the susceptibility to upain-2 or mupain-1 is determined by the exosites, not position 192. In almost all cases, substitution with L-homo-arginine (**6**) either increased or left unchanged the affinity of upain-2 to the uPA variants, but decreased the affinity of mupain-1, whereas the reverse was true for substitutions with amino acids **12** and **16**. Strikingly, the latter P1 substitutions even resulted in a measurable affinity of mupain-1 to wt human uPA and human uPA Q192K, which were not

TABLE 1

K_i values for inhibition of human uPA by upain-2 with P1 substitutions or inhibition of murine uPA by or mupain-1 variants with P1 substitutions
 K_i values for the inhibition of S-2444 hydrolysis by human uPA by the indicated peptides were determined at 37°C. The table shows mean \pm S.D., with the number of determinations indicated in parentheses.

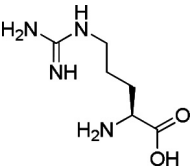
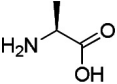
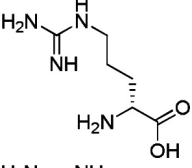
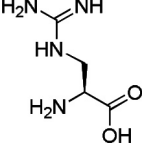
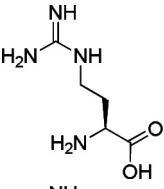
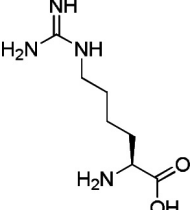
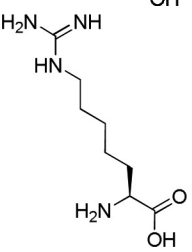
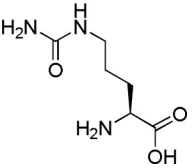
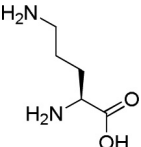
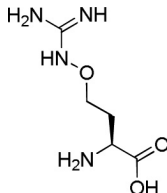
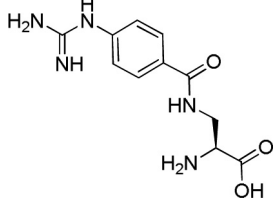
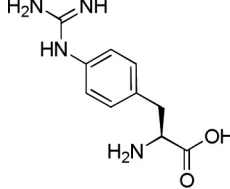
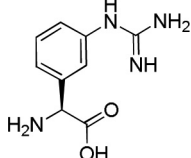
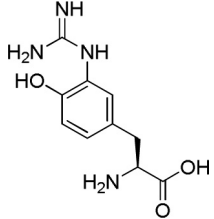
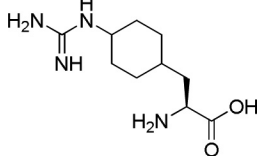
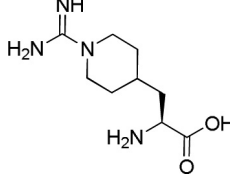
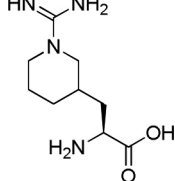
| P1 Residue | Chemical Structure of P1 Residue | K_i for Inhibition | |
|---|---|-----------------------------|-------------------------------|
| | | Human uPA: Upain-2 Variants | Murine uPA: Mupain-1 Variants |
| | | μM | |
| L-Arginine (1) |  | 35 ± 8 (5) | 0.55 ± 0.08 (8) |
| L-Alanine (2) |  | $>1000^{**}$ | $>1000^{***}$ |
| D-Arginine (3) |  | $>1000^{**}$ | $>1000^{***}$ |
| L-2,3-Diaminopropionic acid-amidine (4) |  | $>1000^{**}$ | $>1000^{***}$ |
| L-Nor-arginine (5) |  | $>1000^{**}$ | $>1000^{***}$ |
| L-Homo-arginine (6) |  | 23 ± 4 (3)* | 2.88 ± 0.58 (5)*** |
| L-Bis-homo-arginine (7) |  | $>1000^{**}$ | N.D. |
| L-Citrulline (8) |  | $>1000^{**}$ | $>1000^{***}$ |
| L-Ornithine (9) |  | $>1000^{**}$ | $>500^{***}$ |

TABLE 1—Continued

| P1 Residue | Chemical Structure of P1 Residue | K_i for Inhibition | |
|--|---|-----------------------------|-------------------------------|
| | | Human uPA: Upain-2 Variants | Murine uPA: Mupain-1 Variants |
| | | μM | |
| Canavanine (10) |  | >1000** | 169 ± 9 (3)*** |
| L-4-Guanidino-benzoic acid-2,3-diaminopropionic acid (11) |  | >1000** | >1000*** |
| L-4-Guanidino-phenylalanine (12) |  | >500** | 0.29 ± 0.02 (5)*** |
| L-3-Guanidino-phenylglycine (13) |  | 316 ± 10 (3)** | 343 ± 26 (3)***, ^a |
| L-3-Guanidino-tyrosine (14) |  | >1000** | 396 ± 35 (3)*** |
| L-4-Guanidino-cyclohexyl-alanine (15) |  | >1000** | 0.92 ± 0.25 (3)*** |
| L-3-(N-Amidino-4-piperidyl)alanine (16) |  | >1000** | 0.045 ± 0.010 (4)*** |
| L-3-(N-Amidino-3-piperidyl)alanine (17) |  | N.D. | 3.00 ± 0.34 (3)*** |

N.D., not determined.

^a Two peptides could be isolated with the same mass, probably stemming from epimerization of the sensitive benzylic carbon. The other peptide had no measurable activity.* Significantly different from the K_i values for inhibition of human uPA by upain-2 ($P < 0.05$).** Significantly different from the K_i values for inhibition of human uPA by upain-2 ($P < 0.005$).*** Significantly different from the K_i values for inhibition of murine uPA by mupain-1 ($P < 0.005$).

X-Ray Crystal Structure Analysis of a Complex between a Upain-2 Variant and Human uPA. This analysis

Murine uPAs with human 37 and 60 loops have the mutations Q35R, K36R, N37H, K37aR, Q60aD, L60bY, N63D, and Y99H. The K_i values for the inhibition of S-2444 hydrolysis by human uPA or murine uPA by the indicated peptides were determined at 37°C. The table shows means \pm S.D. for the indicated number of determinations in parentheses. Some data for the human and murine wt enzymes also shown in Table 1 are included to facilitate comparison.

| Original Peptide and PI Residue | Human | | Murine | | | | wt |
|--|-------------------------------|--------------------------------|--------------------------------|---------------------------------------|--------------------------------|---|----------------------------------|
| | uPA H99Y | uPA Q192K | uPA H99Y-Q192K | uPA Y99H, Human 37 and 60 loops | uPA K192Q | uPA Y99H K192Q, Human 37 and 60 Loops | |
| μM | | | | | | | |
| Upain-2 | | | | | | | |
| L-Arginine (1) | >1000 ^{***} | 77 ± 3 (3) ^{***} | >500 ^{*,†} | 287 ± 124 (4) ^{***} | >1000 ^{***} | 351 ± 131 (3) ^{***} | >1000 ^{***} |
| L-Homo-arginine (6) | >500 ^{***} | 17.2 ± 0.8 (3) ^{***} | 156 ± 56 (3) ^{***} | >500 ^{***} | 432 ± 111 (3) ^{***} | 313 ± 126 (3) ^{***} | >1000 ^{***} |
| L-4-Guanidino- | >500 ^{***} | >500 [†] | >1000 [†] | >500 ^{***} | 479 ± 190 (6) ^{***} | 285 ± 83 (4) ^{***} | >500 [†] |
| phenylalanine (12) | | | | | | | |
| L-3-(N-Amidino-4- piperidyl)alanine (16) | >1000 ^{***} | >500 | >1000 ^{***,†} | >1000 ^{***} | >500 [†] | >1000 ^{***} | 382 ± 38 (3) ^{***} |
| Mupain-1 | | | | | | | |
| L-Arginine (1) | 15.3 ± 2.0 (3) ^{***} | >1000 [†] | 9.4 ± 1.3 (3) ^{***} | 21 ± 4 (4) ^{***} | 1.27 ± 0.22 (4) ^{***} | 36 ± 4 (3) ^{***} | 9.7 ± 1.6 (3) ^{***} |
| L-Homo-arginine (6) | >1000 | >1000 [†] | 72 ± 17 (3) ^{***} | 14 ± 1 (4) ^{***} | 11 ± 3 (3) ^{***} | 66 ± 25 (3) ^{***} | 46.2 ± 1.5 (3) ^{***} |
| L-4-Guanidino- | 93 ± 19 (3) [†] | 1.86 ± 0.74 (3) ^{***} | 1.71 ± 0.96 (3) ^{***} | 1.2 ± 0.3 (3) ^{***} | 0.35 ± 0.15 (3) ^{***} | 1.25 ± 0.38 (3) ^{***} | 285 ± 12 (3) ^{***} |
| phenylalanine (12) | | | | | | 34 ± 3 (3) ^{***} | 34 ± 3 (3) ^{***} |
| L-3-(N-Amidino-4- piperidyl)alanine (16) | 93 ± 18 (4) [†] | 2.48 ± 0.07 (3) ^{***} | 1.04 ± 0.13 (3) ^{***} | 1.1 ± 0.1 (3) ^{***} | 0.24 ± 0.04 (3) ^{***} | 2.40 ± 0.65 (3) ^{***} | 0.77 ± 0.02 (3) ^{***} |
| | | | | | | 31 ± 3 (3) ^{***} | 0.045 ± 0.010 (4) ^{***} |

* Significantly different from the K_1 value for mupain-1 ($P < 0.01$).
 ** Significantly different from the K_1 values for upain-2 ($P < 0.01$).
 *** Significantly different from the K_1 values for human wt uPA ($P < 0.01$).
 † Significantly different from the K_1 values for murine wt uPA ($P < 0.01$).

was followed by X-ray crystal structure analysis. However, we were restricted to analyzing complexes between human uPA and upain-2 variants, because it has not yet been possible to crystallize complexes between mupain-1 and murine uPA. Among the complexes between human uPA and upain-2 variants, we were now able to determine the crystal structure of human uPA in complex with an upain-2 analog (upain-2-**13**) to a high resolution (1.32 Å) (Fig. 4A). Peptide upain-2-**13** has a 10-fold lower affinity to human uPA than upain-2 (Table 1).

Structural analysis revealed that the uPA moiety of the uPA-upain-2-**13** complex has a conformation almost identical to that of uPA in complex with the original upain-1 (Zhao et al., 2007) (root mean square deviation of 0.35 Å). Furthermore, the guanidino group of **13** forms five hydrogen bonds with uPA residues in the S1 pocket. This hydrogen bonding scheme is similar, although not identical, to that of the P1 L-Arg in the complex between uPA and upain-1 (Zhao et al., 2007) (Fig. 3). In the uPA-upain-2-**13** complex, the guanidino group aligns well with the carboxyl group of Asp189, allowing the formation of two bifurcated hydrogen bonds between

these structures. In addition, in this complex, the N^{ϵ} atom is hydrogen-bonded to Gly219 (Fig. 3B). In the uPA-upain-1 complex, only one of the N^{η} atoms of the guanidino group hydrogen bonds with Asp189, whereas the other N^{η} hydrogen bonds with Gly219. The contact surface areas in the S1 pocket in the upain-1 complex and the uPA-upain-2-**13** complex are quite similar to each other (150 versus 154 Å²). Thus, the P1-S1 interaction in the uPA-upain-2-**13** complex is similar to that of the uPA-upain-1 complex; however, the guanidino group in the uPA-upain-2-**13** complex probably has a more favorable hydrogen bonding pattern than that in the uPA-upain-1 complex.

In contrast to this conservation of P1-S1 interaction, the P3-P1' segments are quite different in the uPA-upain-2-**13** complex and uPA-upain-1 complex. In the structure of uPA-upain-2-**13**, the peptide is moved toward the solvent and away from uPA by approximately 1.7 Å compared with upain-1 (Fig. 3C). As a result, upain-2-**13** has lost an intramolecular hydrogen bond (Trp3 to Ala6), which exists in upain-1. In addition, Trp3 in the uPA-upain-2-**13** complex makes less contact with uPA compared with that in the uPA-upain-1 complex (64 versus 82 Å²), suggesting a potentially nonoptimal interaction of the inhibitor with uPA. However, the contacts between upain-2-**13** and the exosites in the N-terminal β -barrel remain unchanged. Thus, the anchoring of this peptide in the S1 pocket and to the N-terminal β -barrel exosites leads to a change of the P3-P1' segment and weakening of the interactions of Trp3 with uPA. This result is in agreement with hypothesis 2.

Of importance, both the uPA-upain-1 complex and the uPA-upain-2-**13** complex display decisive differences from the recently determined Michaelis complex between S195A uPA and its natural proteinaceous serpin inhibitor PAI-1 (Lin et al., 2011). In the uPA-PAI-1 Michaelis complex, the P2-P1' sequence inserts into the active site of uPA in a substrate-like fashion. Although the hydrogen bonding scheme of the P1 residue in the uPA-PAI-1 Michaelis complex is similar to that in the uPA-upain-1 complex and the uPA-upain-2-**13** complex, the localizations of the P2 and P1' residues are decisively different. The difference is caused by the inability of the bulky Trp residue in the P2 position of the inhibitory peptides to insert into the S2 pocket of uPA (Fig. 3B) and explains why upain-1 and upain-2-**13** are unable to align into the active site in a substrate-like fashion, whereas PAI-1 is.

Discussion

We here report data elucidating the relative importance of active site and exosite interactions for the binding of peptidyl inhibitors to uPA. The data presented show that exosite interactions strongly influence the effect of a certain P1 substitution on the K_i values. From the data, it seems reasonable to conclude that there is a mutual dependence between the strength of the exosite interactions and the exact fit of the P1 residue into the S1 pocket, thus determining whether a certain P1 substitution affects the affinity positively or negatively. The determination of the K_i values was supplemented by X-ray crystal structure analysis of a upain-2 variant in complex with human uPA, demonstrating that the key to the effect of the P1 substitutions in upain-2 is the communication between the P1-S1 interactions and the interactions of the

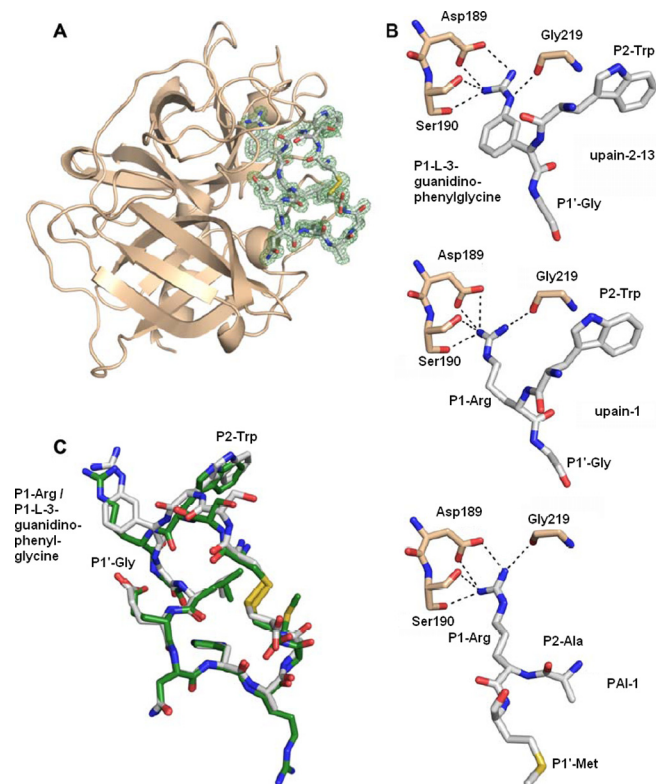


Fig. 3. X-ray crystal structure analysis of the complex between human uPA and upain-2-**13**. A, overview of the complex between human uPA and upain-2-**13**. The uPA structure is shown as ribbons and upain-2-**13** is indicated in sticks with CPK colors. The electron density map (σ -weighted $2F_o - F_c$ omit map contoured at 1.0 σ) of upain-2-**13** is shown in green. B, close-ups of the interactions of the P1 residues of various inhibitors within the S1 pocket of uPA. Top, uPA-upain-2-**13** complex; middle, uPA-upain-1 complex (PDB file [2NWN](#)) (Zhao et al., 2007); bottom, PAI-1-uPA Michaelis complex (PDB file [3PB1](#)) (Lin et al., 2011). Besides the P1 residues of the inhibitors, the figure also shows the P2 residues (Trp in upain-2-**13** and upain-1 and Ala in PAI-1) and the P1' residues (Gly in upain-2-**13** and upain-1 and Met in PAI-1) of the inhibitors and Asp189, Ser190, and Gly219 of uPA. C, comparison of the structures of upain-2-**13** and upain-1 in their complexes with uPA. The figure was constructed by aligning the uPA moieties of the complexes. Upain-2-**13** is shown in sticks with CPK colors and upain-1 is in green.

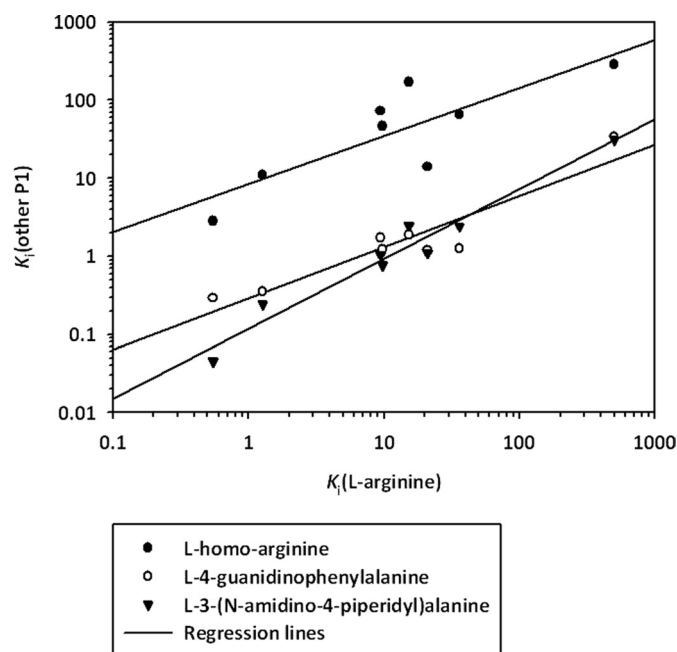


Fig. 4. The relationship between the K_i values for mupain-1 substituted with non-natural amino acids and the K_i values for mupain-1. The figure is based on the K_i values presented in Table 2 for wt human and murine uPA and human-murine uPA chimeras. Data points corresponding to K_i values more than 500 μM were omitted.

Trp3 of upain-2. Taken together, the data are in agreement with the above formulated hypothesis 2 rather than hypothesis 1.

Searching for quantitative patterns in the changes in K_i values after substitution of the P1 L-Arg with non-natural amino acids, we plotted the K_i values for inhibition of the various uPA variants by the various non-natural mupain-1 variants versus the corresponding values for the original mupain-1 in a double logarithmic plot (Fig. 4). A similar plot could not be constructed for upain-2, because the K_i values were in too many cases above the level allowing an accurate determination. With the mupain-1 variants, we observed a linear relationship in such a plot (Fig. 4). Although there is no obvious molecular explanation for the linearity of the plot, it does allow us to draw an interesting inference about the effect of the substitutions. With both L-homo-arginine (**6**) and the Phe analog **12**, the slopes of the lines were less than 1 (0.62 and 0.66, respectively), indicating that P1 substitutions with these amino acids generally caused more increase or less decrease in affinity, the lower the affinity of the original mupain-1 peptide was to the target enzyme. However, with the amidino compound **16**, the slope was 0.89, showing that the fold change in K_i was almost independent of the target. On the basis of this observation, one may suggest that the effect of the substitutions also partly depends on a target-independent element. This dependence cannot be explained by either hypothesis 1 or hypothesis 2 but may rather be related to a destabilization of the unbound state of the peptide.

Comparison of the roles of murine and human uPA in xenografted tumors may help to delineate the relative importance of tumor and host uPA in tumor growth and spread. Availability of species-specific inhibitors is therefore important. Although a number of inhibitors of human uPA have been developed, the species specificity has been studied in only a few cases. Species-specific inhibitory polyclonal and

monoclonal antibodies (Danø et al., 1980; Kaltoft et al., 1982; Petersen et al., 2001; Lund et al., 2008; Blouse et al., 2009) are available but lack some of the advantageous properties of peptides. Some aryl-amidine-based, small molecule inhibitors had a strong preference (up to 203-fold) for human uPA over murine uPA (Klinghofer et al., 2001). Whereas naphthamidine targeted only the S1 pocket and was equally potent with human and murine uPA, the specificity for human uPA increased with increasing number and increasing size of the side chains. X-ray crystal structure analysis demonstrated that the most specific inhibitors interacted with Asp60a in human uPA, but no mutagenesis was performed to test this suggestion. Nevertheless, the observation is in agreement with our finding that specificity depends on exosite interactions (Fig. 2) (Hansen et al., 2005; Zhao et al., 2007; Andersen et al., 2008).

The strong species specificities of upain-2 and mupain-1 depend on the interaction of the peptides with species-specific surface loops outside the active site (Fig. 2). Human or murine uPA can be made susceptible to mupain-1 or upain-2 by grafting mouse-specific residues onto human uPA or human-specific residues onto murine uPA (Table 2). In this context, one also notes that substitution of the P1 L-Arg residue with the amidino compound **16**, L-homo-arginine (**6**), or the Phe derivative **12** may deteriorate the species specificity. This could be due to a larger fraction of the binding energy depending on interactions within the S1 pocket or other target-independent contributions. Several examples illustrate this point. Thus, the original mupain-1 is a >2000-fold better inhibitor of murine uPA than of human uPA, but mupain-1-**12** is only a 300-fold better inhibitor of murine uPA than of human uPA. Nevertheless, mupain-1-**16**, the best mupain-1 variant developed until now, still displays an approximately 2000-fold selectivity for murine uPA over human uPA. This high specificity could indicate that mupain-1-**16** also will be specific among serine proteases in general, which, combined with a favorable K_i (45 nM), makes mupain-1-**16** a candidate for use in in vivo experiments.

Authorship Contributions

Participated in research design: Sørensen, K. J. Jensen, Hosseini, Huang, and Andreasen.

Conducted experiments: Yuan, Sørensen, Hosseini, Jiang, Christensen, and J. K. Jensen.

Contributed new reagents or analytic tools: Sørensen, Andersen, Hosseini, and Fogh.

Performed data analysis: K. J. Jensen, Hosseini, Huang, Andreasen, Sørensen, Christensen, and J. K. Jensen.

Wrote or contributed to the writing of the manuscript: K. J. Jensen, Hosseini, Huang, Andreasen, Sørensen, and J. K. Jensen.

References

- Abramowitz N, Schechter I, and Berger A (1967) On the size of the active site in proteases. II. Carboxypeptidase-A. *Biochem Biophys Res Commun* **29**:862–867.
- Andersen LM, Wind T, Hansen HD, and Andreasen PA (2008) A cyclic peptidyl inhibitor of murine urokinase-type plasminogen activator: changing species specificity by substitution of a single residue. *Biochem J* **412**:447–457.
- Andreasen PA, Egelund R, and Petersen HH (2000) The plasminogen activation system in tumor growth, invasion, and metastasis. *Cell Mol Life Sci* **57**:25–40.
- Blouse GE, Dupont DM, Schar CR, Jensen JK, Minor KH, Anagli JY, Gårdsvoll H, Ploug M, Peterson CB, and Andreasen PA (2009) Interactions of plasminogen activator inhibitor-1 with vitronectin involve an extensive binding surface and induce mutual conformational rearrangements. *Biochemistry* **48**:1723–1735.
- Boyar A and Marsh RE (1982) L-Canavanine, a paradigm for the structures of substituted guanidines. *J Am Chem Soc* **104**:1995–1998.
- Branden C and Tooze J (1991) *Introduction to Protein Structure*. Garland Publishing, New York.

- Collaborative Computational Project, Number 4 (1994) The CCP4 suite: programs for protein crystallography. *Acta Crystallogr D Biol Crystallogr* **50**:760–763.
- Danø K, Nielsen LS, Møller V, and Engelhart M (1980) Inhibition of a plasminogen activator from oncogenic virus-transformed mouse cells by rabbit antibodies against the enzyme. *Biochim Biophys Acta* **630**:146–151.
- DeLano (2002) *The PyMOL Molecular Graphics System*, San Carlos, CA.
- Dennis MS, Eigenbrot C, Skelton NJ, Ultsch MH, Santell L, Dwyer MA, O'Connell MP, and Lazarus RA (2000) Peptide exosite inhibitors of factor VIIa as anticoagulants. *Nature* **404**:465–470.
- Emsley P and Cowtan K (2004) Coot: model-building tools for molecular graphics. *Acta Crystallogr D Biol Crystallogr* **60**:2126–2132.
- Hajdin K, D'Alessandro V, Niggli FK, Schäfer BW, and Bernasconi M (2010) Furin targeted drug delivery for treatment of rhabdomyosarcoma in a mouse model. *PLoS One* **5**:e10445.
- Hansen M, Wind T, Blouse GE, Christensen A, Petersen HH, Kjølgaard S, Mathiasen L, Holtet TL, and Andreasen PA (2005) A urokinase-type plasminogen activator-inhibiting cyclic peptide with an unusual P2 residue and an extended protease binding surface demonstrates new modalities for enzyme inhibition. *J Biol Chem* **280**:38424–38437.
- Hartung R, Hitzel-Zerrahn F, Müller T, and Pietsch J (2005) inventors; Degussa AG, assignee. Process for the hydrogenation of aromatic compounds. World patent WO/2005/014526. 2005 Feb 17.
- Hedstrom L (2002) Serine protease mechanism and specificity. *Chem Rev* **102**:4501–4524.
- Heinis C, Rutherford T, Freund S, and Winter G (2009) Phage-encoded combinatorial chemical libraries based on bicyclic peptides. *Nat Chem Biol* **5**:502–507.
- Hekim C, Leinonen J, Närvalä A, Koistinen H, Zhu L, Koivunen E, Väisänen V, and Stenman UH (2006) Novel peptide inhibitors of human kallikrein 2. *J Biol Chem* **281**:12555–12560.
- Jorgensen L and Nielsen HM (2009) *Delivery Technologies for Biopharmaceuticals Peptides, Proteins, Nucleic Acids and Vaccines*. John Wiley & Sons, Chichester, UK.
- Kaltoft K, Nielsen LS, Zeuthen J, and Danø K (1982) Monoclonal antibody that specifically inhibits a human M_r 52,000 plasminogen-activating enzyme. *Proc Natl Acad Sci USA* **79**:3720–3723.
- Kayser KJ, Glenn MP, Sebt SM, Cheng JQ, and Hamilton AD (2007) Modifications of the GSK3 β substrate sequence to produce substrate-mimetic inhibitors of Akt as potential anti-cancer therapeutics. *Bioorg Med Chem Lett* **17**:2068–2073.
- Klinghofer V, Stewart K, McGonigal T, Smith R, Sarthy A, Nienaber V, Butler C, Dorwin S, Richardson P, Weitzberg M, et al. (2001) Species specificity of amidine-based urokinase inhibitors. *Biochemistry* **40**:9125–9131.
- Kocsis A, Kékesi KA, Szász R, Végh BM, Balczér J, Dobó J, Závodszy P, Gál P, and Pál G (2010) Selective inhibition of the lectin pathway of complement with phage display selected peptides against mannose-binding lectin-associated serine protease (MASP)-1 and -2: significant contribution of MASP-1 to lectin pathway activation. *J Immunol* **185**:4169–4178.
- Krook M, Lindblad C, Eriksen JA, and Mosbach K (1997–1998) Selection of a cyclic nonapeptide inhibitor to α -chymotrypsin using a phage display peptide library. *Mol Divers* **3**:149–159.
- Lin Z, Jiang L, Yuan C, Jensen JK, Zhang X, Luo Z, Furie BC, Furie B, Andreasen PA, and Huang M (2011) Structural basis for recognition of urokinase-type plasminogen activator by plasminogen activator inhibitor-1. *J Biol Chem* **286**:7027–7032.
- Lund IK, Jögi A, Rønø B, Rasch MG, Lund LR, Almholzt K, Gårdsvoll H, Behrendt N, Rømer J, and Høyer-Hansen G (2008) Antibody-mediated targeting of the urokinase-type plasminogen activator proteolytic function neutralizes fibrinolysis in vivo. *J Biol Chem* **283**:32506–32515.
- Otwinski Z and Minor W (1997) Processing of X-ray diffraction data collected in oscillation mode. *Methods Enzymol* **276**:307–326.
- Petersen HH, Hansen M, Schousboe SL, and Andreasen PA (2001) Localization of epitopes for monoclonal antibodies to urokinase-type plasminogen activator—relationship between epitope localization and effects of antibodies on molecular interactions of the enzyme. *Eur J Biochem* **268**:4430–4439.
- Puente XS, Ordóñez GR, and López-Otin (2008) *The Cancer Degradome: Proteases and Cancer Biology*. Springer, New York.
- Rao PN, Peterson DM, Acosta CK, Bahr ML, and Kim HK (1991) Synthesis of cis-4-aminocyclohexyl-D-alanine and trans-4-aminocyclohexyl-D-alanine derivatives and determination of their stereochemistry. *Org Prep Proced Int* **23**:103–110.
- Rockway TW, Nienaber V, and Giranda VL (2002) Inhibitors of the protease domain of urokinase-type plasminogen activator. *Curr Pharm Des* **8**:2541–2558.
- Sassatelli M, Debiton E, Aboab B, Prudhomme M, and Moreau P (2006) Synthesis and antiproliferative activities of indolin-2-one derivatives bearing amino acid moieties. *Eur J Med Chem* **41**:709–716.
- Spraggon G, Phillips C, Nowak UK, Ponting CP, Saunders D, Dobson CM, Stuart DI, and Jones EY (1995) The crystal structure of the catalytic domain of human urokinase-type plasminogen-activator. *Structure* **3**:681–691.
- Walker B and Lynas JF (2001) Strategies for the inhibition of serine proteases. *Cell Mol Life Sci* **58**:596–624.
- Wu P, Leinonen J, Koivunen E, Lankinen H, and Stenman UH (2000) Identification of novel prostate-specific antigen-binding peptides modulating its enzyme activity. *Eur J Biochem* **267**:6212–6220.
- Wu P, Weisell J, Pakkala M, Peräkylä M, Zhu L, Koistinen R, Koivunen E, Stenman UH, Närvalä A, and Koistinen H (2010) Identification of novel peptide inhibitors for human trypsin. *Biol Chem* **391**:283–293.
- Zhao G, Yuan C, Wind T, Huang Z, Andreasen PA, and Huang M (2007) Structural basis of specificity of a peptidyl urokinase inhibitor, upain-1. *J Struct Biol* **160**:1–10.

Address correspondence to: Dr. Knud J. Jensen, IGM, Faculty of Life Sciences, University of Copenhagen, Thorvaldsensvej 40, 4 sal, Copenhagen, Denmark. E-mail: kjj@life.ku.dk